The Journal of Chemical Physics

A single nucleobase tunes nonradiative decay in a DNA-bound silver cluster

Cite as: J. Chem. Phys. **155**, 094305 (2021); https://doi.org/10.1063/5.0056836
Submitted: 14 May 2021 • Accepted: 12 August 2021 • Published Online: 03 September 2021

Yuyuan Zhang, Chen He, Kimberly de La Harpe, et al.

The Journal of Chemical Physics ARTICLE scitation.org/journal/jcp

A single nucleobase tunes nonradiative decay in a DNA-bound silver cluster

Cite as: J. Chem. Phys. 155, 094305 (2021); doi: 10.1063/5.0056836
Submitted: 14 May 2021 • Accepted: 12 August 2021 •
Published Online: 3 September 2021

Yuyuan Zhang,[1] Chen He,[2] Kimberly de La Harpe,[3] Peter M. Goodwin,[4] Jeffrey T. Petty,[2,a)] and Bern Kohler[1,a)]

AFFILIATIONS

[1] Department of Chemistry and Biochemistry, The Ohio State University, 100 West 18th Avenue, Columbus, Ohio 43210, USA
[2] Department of Chemistry, Furman University, Greenville, South Carolina 29613, USA
[3] Department of Physics, United States Air Force Academy, U.S. Air Force Academy, Colorado 80840, USA
[4] Center for Integrated Nanotechnologies, Los Alamos National Laboratory, Mail Stop K771, Los Alamos, New Mexico 87545, USA

Note: This paper is part of the JCP Special Topic on From Atom-Precise Nanoclusters to Superatom Materials.
[a)] **Authors to whom correspondence should be addressed:** jeff.petty@furman.edu. **Tel.:** +1 864-294-2689 and kohler.40@osu.edu. **Tel.:** +1 614-688-2635

ABSTRACT

DNA strands are polymeric ligands that both protect and tune molecular-sized silver cluster chromophores. We studied single-stranded DNA $C_4AC_4TC_3XT_4$ with X = guanosine and inosine that form a green fluorescent Ag_{10}^{6+} cluster, but these two hosts are distinguished by their binding sites and the brightness of their Ag_{10}^{6+} adducts. The nucleobase subunits in these oligomers collectively coordinate this cluster, and fs time-resolved infrared spectra previously identified one point of contact between the C2–NH_2 of the X = guanosine, an interaction that is precluded for inosine. Furthermore, this single nucleobase controls the cluster fluorescence as the X = guanosine complex is ~2.5× dimmer. We discuss the electronic relaxation in these two complexes using transient absorption spectroscopy in the time window 200 fs–400 μs. Three prominent features emerged: a ground state bleach, an excited state absorption, and a stimulated emission. Stimulated emission at the earliest delay time (200 fs) suggests that the emissive state is populated promptly following photoexcitation. Concurrently, the excited state decays and the ground state recovers, and these changes are ~2× faster for the X = guanosine compared to the X = inosine cluster, paralleling their brightness difference. In contrast to similar radiative decay rates, the nonradiative decay rate is 7× higher with the X = guanosine vs inosine strand. A minor decay channel via a dark state is discussed. The possible correlation between the nonradiative decay and selective coordination with the X = guanosine/inosine suggests that specific nucleobase subunits within a DNA strand can modulate cluster–ligand interactions and, in turn, cluster brightness.

I. INTRODUCTION

Molecular-sized and nanoscale silver clusters are more akin to organic dyes than to the bulk metal.[1–3] Due to their small sizes with sparsely organized valence electronic states, they fluoresce across the optical and near-infrared (NIR) spectral regions, and this emission can be reversibly toggled between bright and dark levels.[4–9] They are typically synthesized by reducing an ionic silver salt, and a nascent cluster can be quickly engulfed by using ligands to coordinate its surface and arrest growth.[10,11] These ligands not only chemically trap but also control the fluorescence of their sequestered clusters.[12] A network of metal–ligand and peripheral intermolecular bonds imprisons a cluster and can thereby tune the cluster's electronic states.[13,14] Ligands can be further organized by covalently linking them together, and we focus on polymeric ligands that coordinate a cluster as a single unit.[15–18]

Single-stranded oligonucleotides are monodisperse polymers that coordinate molecular silver clusters through their nucleobase subunits.[19–21] The four canonical nucleobases have different binding sites and distinct affinities for silver, so their linear sequence along the DNA backbone establishes a specific ligation pattern.[22–24] Furthermore, the strand is able to fold and assemble around a cluster core as its anchoring backbone is flexible.[25–27] Thus, the sequence and structure of a DNA polymer establish a unique binding site for a fluorescent silver cluster. Detailed maps of the coordination sites emerge through visible and x-ray spectroscopy, mass spectrometry,

x-ray crystallography, molecular modeling, and hydrodynamic studies.[22,28–35]

Our studies are motivated by recent time-resolved infrared spectroscopy studies of the $C_4AC_4TC_3XT_4$–Ag_{10}^{6+} with X = guanosine and inosine. These clusters have matching optical spectra as well as stoichiometries and charges (Figs. S1 and S2, respectively) but are distinguished via their transient infrared spectra.[36] When the Ag_{10}^{6+} cluster was selectively photoexcited, the mid-infrared vibrations of the ligated X = guanosine and inosine were perturbed along with cytosines. This is a remarkable selectivity for one of the 18 nucleobases in the strand, given that this single substitution results in indistinguishable steady-state FTIR spectra. These findings suggest that coordination by the C_2–NH_2 of guanosine takes place but is absent for the analogous C_2–H of inosine. The significance of this amino group is further bolstered because the Ag_{10}^{6+} cluster with the X = guanosine vs inosine strand is 2.5× dimmer.[27]

When DNA–silver cluster (DNA-AgC) fluorophores are photoexcited, they can electronically relax through multiple channels on distinct time scales, such as internal conversion to the ground state (<1 ps), emission (<10 ns), and crossing to/from a metastable dark state (<100 μs).[37,38] In the present study, we follow both radiative and nonradiative relaxation from the emissive state in $C_4AC_4TC_3XT_4$–Ag_{10}^{6+} over a nine decade time range via femtosecond- and nanosecond- transient absorption (fs- and ns-TA) spectroscopies. We combine observations from these transient absorption spectra along with time-resolved emission and fluorescence correlation spectroscopy (FCS) studies to identify the key electronic states and relaxation pathways of the photoexcited Ag_{10}^{6+} cluster.

II. EXPERIMENTAL

The DNA-bound silver clusters were synthesized as described previously (see the supplementary material for full discussion).[39] Ag_{10}^{6+} is the only molecular-sized, partially reduced adduct in the mass spectra, and spectroscopic studies suggest that it is formed preferentially.[39]

The fs-TA experiments in the 200 fs–3.5 ns range probed electronic transitions in the UV–visible–NIR region for the DNA–AgC samples (~25 μM DNA–AgC recirculating in a 1 mm path length cell) (see the supplementary material for full discussion). The sample was excited with ~140 fs laser pulses with a center wavelength of 490 nm. A low pump fluence of 0.03 mJ cm^{-2}, corresponding to an average of 0.02 excitons per cluster, was used to minimize degradation and to avoid multiphoton absorption (see Fig. S3 and associated text in the supplementary material). In addition, the low pump fluence minimized scattered pump light and allowed ground state bleach recovery kinetics to be recorded. The instrument response time is ~200 fs (Fig. S4). At t > 200 fs, the composite fs-TA spectra of both AgCs have similar positive and negative transient absorption bands [Figs. 1(a) and 1(b)]. fs-TA signals could not be detected in either sample at longer NIR wavelengths (λ_{probe} = 1000–1350 nm). Nanosecond transient absorption (ns-TA) experiments were performed using a nanosecond laser with a pulse width of 3–5 ns and a Xe arc lamp (see the supplementary material for full discussion) to observe slower relaxation pathways for the electronically excited clusters. The instrument response function (IRF) was ~7 ns.

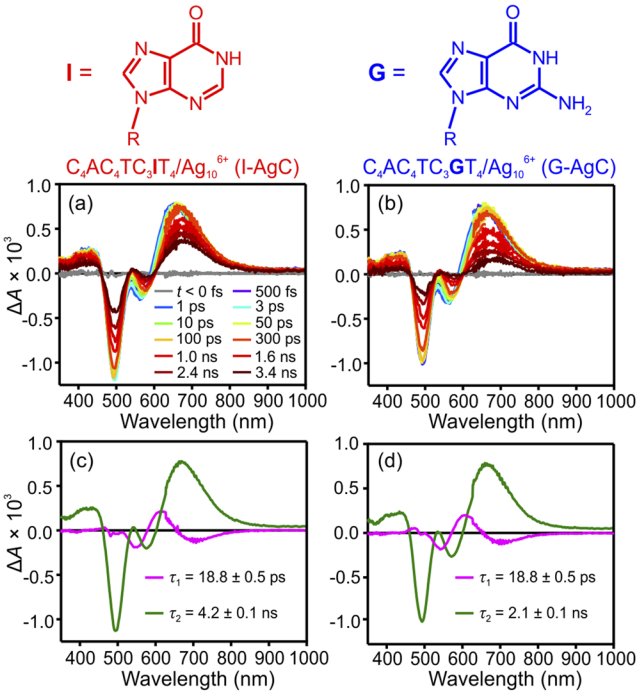

FIG. 1. (a) and (b) Composite fs-TA spectra of I-AgC and G-AgC, respectively, recorded at selected delay times following 490 nm excitation. (c) and (d) Decay-associated difference spectra (DADS, see Ref. 46) of I-AgC and G-AgC, respectively, obtained by globally fitting the TA data from 200 fs to 3.5 ns. Data were fitted to a biexponential decay function $\Delta A(t) = A_1 \exp(-t/\tau_1) + A_2 \exp(-t/\tau_2)$. Uncertainties are reported as 2σ.

III. RESULTS AND DISCUSSION

A. Short time range

The fs-TA spectra from 200 fs to 3.5 ns over the range 300–1000 nm reveal three common bands for the I- and G-AgC complexes (Fig. 1). A band centered at 490 nm coincides with the steady-state absorption peak, and this negative band is assigned to ground state bleaching (GSB) that approaches the ΔA = 0 baseline with time (Fig. 2). The positive absorption with λ_{max} of 660 nm is assigned to excited state absorption (ESA) because this absorption decays in lock steps as the ground state recovers. This correlation suggests that this excited state directly feeds the ground state. Transient near-infrared absorption features have also been observed for other DNA-bound silver clusters.[37,40] A negative-going band starts at 560 nm at 200 fs and shifts to 570 nm by 500 ps, and this band coincides with the steady-state emission band and is assigned to stimulated emission (SE) (Fig. S1). While such emission has been observed for a NIR-emitting Ag_{20}–DNA conjugate at cryogenic temperatures,[41] it is reported here for the first time for a DNA–AgC in aqueous solution at room temperature. The emission appears promptly, so this early snapshot suggests that the emissive state is rapidly populated to develop most of the 2500 cm^{-1} Stokes shift within the ~200 fs IRF of our spectrometer. Reveguk *et al.* attributed an ultrafast decay for their green-emitting DNA–AgC to a geometry change of the AgC core in the excited state.[42] The slow drift

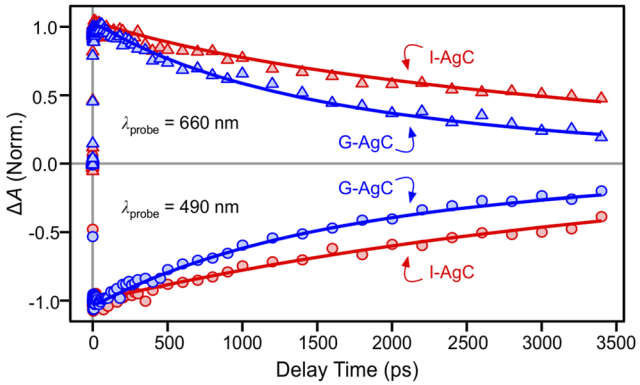

FIG. 2. Kinetic decay traces of I-AgC (red) and G-AgC (blue) with probing at 490 nm (circles) and 660 nm (triangles) from 200 fs to 3.5 ns following 490-nm excitation. The markers are raw data, and the solid traces are best-fit curves obtained from global fitting (see the text). The traces have been normalized to the magnitude of the TA signal at 200 fs. The vertical and horizontal gray lines denote $t = 0$ and $\Delta A = 0$, respectively.

from 560 to 570 nm over its 500 ps range may be attributed to the flexibility of its host. DNA conformation fluctuations are sluggish in relation to solvation dynamics, as indicated by the ps and ns spectral shifts for DNA-bound red- and NIR-emitting silver clusters and DNA-intercalated organic dyes.[35,38,43–45]

Both the steady-state and transient spectra are similar for the two DNA-bound clusters, establishing that the two $C_4AC_4TC_3XT_4$ strands conserve the coordination site for their Ag_{10}^{6+} adducts. However, the two Ag_{10}^{6+} chromophores relax at different rates (Fig. 2). When monitoring both the 490 nm GSB and the 660 nm ESA, the I-AgC complex returns to the ground state nearly monoexponentially with a 4.2 ± 0.1 ns lifetime. This decay time accounts for 97% of the ground state repopulation with the 3% balance of 18.8 ± 0.5 ps attributed to time-dependent shifts in the SE and ESA bands [Fig. 1(c)]. In contrast, the photoexcited G-AgC complex relaxes twice as rapidly with a 2.1 ± 0.2 ns time constant (98%) and an analogous 18.8 ± 0.5 ps component (2%) [Fig. 1(d)]. These transient absorption lifetimes match the amplitude-weighted fluorescence lifetimes (Table I), independently supporting relaxation from the emissive excited state back to the ground state. We note

TABLE I. Dominant decay component, τ_2, from fs-TA experiments, the amplitude-weighted emission lifetime, $\langle\tau\rangle$, and the estimated radiative lifetime, τ_r, and nonradiative lifetime, τ_{nr}, for the studied silver clusters.

	τ_2 (ns)[a]	$\langle\tau\rangle$ (ns)[b]	τ_r (ns)[c]	τ_{nr} (ns)[d]
I-AgC	4.2 ± 0.2	3.4 ± 0.1	5.4 ± 0.2	19 ± 5
G-AgC	2.1 ± 0.2	1.9 ± 0.3	7.6 ± 1.9	2.9 ± 0.5

[a] $\lambda_{pump} = 490$ nm.
[b] Amplitude-weighted lifetimes were calculated by $\langle\tau\rangle = \sum_i A_i\tau_i / \sum_i A_i$. Lifetimes and amplitudes are from fits to time-correlated single-photon counting (TCSPC) emission measurements with $\lambda_{ex} = 470$ nm, $\lambda_{em} = 525$ nm. Values are from Table 2 in Ref. 27.
[c] Radiative lifetimes were calculated by $\tau_r = \langle\tau\rangle / Q_F$ using fluorescence quantum yield, Q_F, values from Table 2 in Ref. 27.
[d] Time constants for nonradiative decay were calculated by $\tau_{nr}^{-1} = k_{nr} = \tau_2^{-1} - \tau_r^{-1}$.

that after ~100 ps, the transient decays are monoexponential, while the fluorescence decays are biexponential. The latter may result from monitoring the decay on the blue side of the fluorescence maximum, and/or the greater sensitivity and the extended time window of the time-correlated single-photon counting (TCSPC) vs fs-TA measurements (200 vs 3.5 ns).[38,43] The fs-TA data were also analyzed by fitting with an offset to look for decay pathways beyond our 3.5 ns limit (Fig. S5 and Table S1 in the supplementary material). The small offset amplitudes of 6% for I-AgC and 14% for G-AgC (Table S1) indicate that most of the fs-TA signal at 490 nm (GSB) decays on a nanosecond time scale, with G-AgC again decaying faster (2.3×) than I-AgC. More definitive evidence for a long-lived state is provided by ns-TA and fluorescence correlation measurements, which are described next.

B. Long time range

The ns-TA experiments show a GSB at 490 nm, and its kinetics were probed via two time windows—up to 1.6 μs with 0.2 ns resolution and up to 400 μs with 40 ns resolution. The shorter window shows a constant offset, thus substantiating the offset in our fs-TA fits [Figs. 3(a) and S6]. In our longer time window, this offset evolves into a biexponential decay with 20 μs (G-AgC)/25 μs (I-AgC) and $\gtrsim$400 μs (G-AgC and I-AgC) lifetimes [Fig. 3(b)]. Such longer lifetimes of 1–100 μs have been observed for metastable states of other DNA–silver complexes.[37,40,47,48]

The prompt ns-TA signals ($t < 20$ ns) are a convolution of not only the recovery of the ground state but also the fluorescence from the emissive state. Furthermore, these decay faster than the 7.4 ns IRF. To address this limitation, we used the excitation conditions of the ns-TA experiments to estimate the initial GSB signal in our fs-TA experiments and then compared it with the amplitude of the long-lived state. This shows that roughly 4% of the excited-state population traps to the μs state for both I- and G-AgC (see the supplementary material for full details). This quantum yield is consistent with studies of other DNA-bound clusters[37,47,49] and with the offsets in our ns-TA fits.

Fluorescence correlation spectroscopy independently supports a μs-lived state for the G-AgC complex. This technique monitors the fluctuations in the emission from a small number of molecules in an fL probe volume, and two components are resolved in the autocorrelation analysis (Fig. S7). First, the emission fluctuates because the DNA–cluster complexes freely diffuse through the open, confocally defined probe volume, and the time constant of ~260 μs is consistent with the hydrodynamic radii of DNA–silver cluster complexes.[39] The corresponding diffusion coefficient of 97 μm^2/s and hydrodynamic volume of 45 nm^3 are consistent with earlier studies.[27] Second, the emission blinks if these fluorophores cross to a metastable dark electronic state, and the time constant of ~17 μs measured for G-AgC agrees with the decay time of 20 μs measured in the ns-TA experiment, thus further supporting shelving to a μs-lived electronic state [see Fig. 4(b) of Ref. 37].

C. Photophysical model

As photoexcited $C_4AC_4TC_3XT_4/Ag_{10}^{6+}$ complexes have a low dark state quantum yield of 4% (see the supplementary material) and

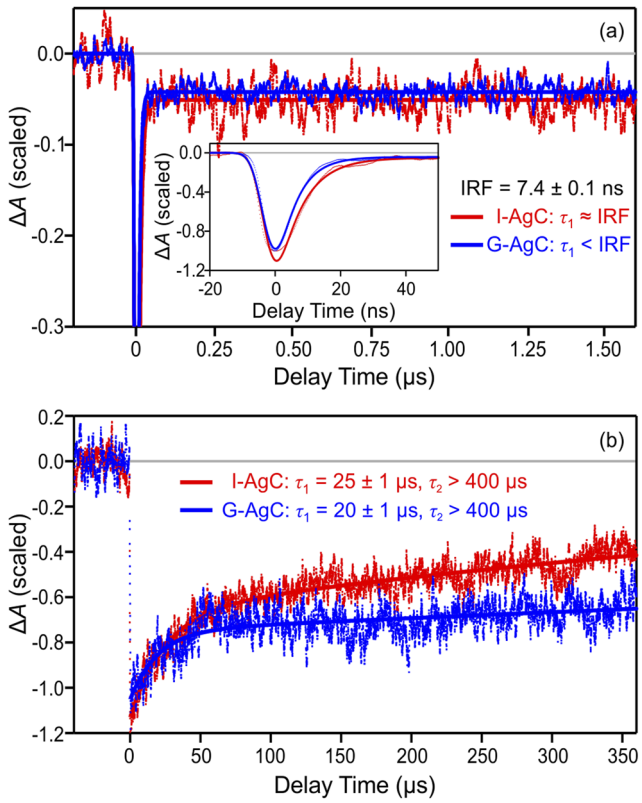

FIG. 3. Normalized GSB kinetics of I-AgC (red) and G-AgC (blue) probed at 492 nm after 490 nm excitation, up to 1.6 μs with a step size of 0.2 ns (a) and up to 400 μs with a step size of 40 ns (b). The dots are the experimental data, and the solid lines are best–fit curves. The curves in panel (a) were fit to a monoexponential decay function plus an offset, $\Delta A(t) = A_1 \exp(-t/\tau_1) + A_2$, convoluted with a normalized Gaussian function. The curves in panel (b) were fit to a biexponential decay function $\Delta A(t) = A_1 \exp(-t/\tau_1) + A_2 \exp(-t/\tau_2)$. Uncertainties are reported as 2σ.

because the fluorescence quantum yields of I-AgC and G-AgC are 63% and 25%, respectively, we propose that the additional nonradiative relaxation from the fluorescent state competes with emission. This competition reveals the key distinction between the complexes (Table I). While the radiative rates are similar, the nonradiative decay rate is nearly sevenfold higher for G-AgC than for I-AgC. The brightness and suppressed nonradiative decay rate of I-AgC could imply a weaker interaction between the inosine and the metal cluster due to the missing C2–NH_2 group. The key question is whether this is a causative relationship, that is, does DNA–cluster coordination control nonradiative relaxation? One possibility is that tight coordination facilitates orbital overlap, which in turn promotes charge transfer and nonradiative relaxation.[50] Charge transfer and electron donation control the electronic stability and photoluminescence of ligated noble-metal nanoclusters.[37,51,52] Mixed ligand and metal electronic states with charge transfer character have been proposed for atomically precise silver clusters bound to thiolate ligands.[53,54] A charge transfer state involving the ligand and the metal core is also predicted for DNA–AgC via theoretical calculations.[55,56]

The metastable dark state is a minor sink following photoexcitation, but our fs-TA, ns-TA, and FCS studies indirectly identify this state because it hinders the ground state recovery. This state was further characterized by using aerated and deaerated solutions, and these yield identical signals in the 0–200 ns window of our ns-TA measurements (Fig. S6). The absence of quenching by oxygen nominally argues against triplet states, but it is possible that the encapsulating DNA strands inhibit dissolved O_2 from reaching the cluster and quenching triplet states as seen when triplet emitters are encapsulated in cyclodextrins or other supramolecular structures.[35,57]

IV. CONCLUSION

The two $C_4AC_4TC_3GT_4$-Ag_{10}^{6+} complexes with X = G and I are nearly identical—the clusters have matching stoichiometries, oxidation states, and absorption/emission spectra. However, the guanosine strand is dimmer and has a 2.5× lower fluorescence quantum yield and a 1.8× shorter fluorescence lifetime than its inosine counterpart. While the two complexes have similar radiative lifetimes, the G-AgC cluster has a sevenfold more efficient nonradiative channel connecting the emissive state with the ground state in relation to the I-AgC cluster. Thus, the brightness of this DNA–AgC was modulated by a single-site mutation without compromising the structure of the cluster. Targeted changes to nucleobases that bind strongly to a given metal cluster suggest that cluster brightness can be tuned via the DNA scaffold.

SUPPLEMENTARY MATERIAL

See the supplementary material for the synthesis and characterization of the silver clusters, experimental methods for the steady-state emission spectroscopy, broadband fs-TA, ns-TA, and fluorescence correlation spectroscopy.

ACKNOWLEDGMENTS

The work at Ohio State University was supported by the U.S. National Science Foundation (Grant No. CHE-1800471) and by funding from Ohio State University. The work at Furman was supported by the National Science Foundation (Grant Nos. CHE-1611451 and CHE-2002910) and the Furman Advantage Program. This work was supported, in part, by the National Science Foundation EPSCoR Program under NSF Award No. OIA-1655740. This work was performed, in part, at the Center for Integrated Nanotechnologies, an Office of Science User Facility operated for the U.S. Department of Energy (DOE) Office of Science by Los Alamos National Laboratory (Contract No. 89233218CNA000001) and Sandia National Laboratories (Contract No. DE-NA-0003525).

DATA AVAILABILITY

The data that support the findings of this study are available within this article and its supplementary material.

REFERENCES

[1] R. Kubo, J. Phys. Soc. Jpn. **17**(6), 975–986 (1962).
[2] R. Kubo, A. Kawabata, and S.-I. Kobayashi, Annu. Rev. Mater. Sci. **14**(1), 49–66 (1984).

[3]J. Zheng, P. R. Nicovich, and R. M. Dickson, Annu. Rev. Phys. Chem. **58**, 409–431 (2007).
[4]W. Schulze, I. Rabin, and G. Ertl, ChemPhysChem **5**(3), 403–407 (2004).
[5]C. I. Richards, S. Choi, J.-C. Hsiang, Y. Antoku, T. Vosch, A. Bongiorno, Y.-L. Tzeng, and R. M. Dickson, J. Am. Chem. Soc. **130**(15), 5038–5039 (2008).
[6]S. M. Swasey, S. M. Copp, H. C. Nicholson, A. Gorovits, P. Bogdanov, and E. G. Gwinn, Nanoscale **10**(42), 19701–19705 (2018).
[7]H.-C. Yeh, J. Sharma, J. J. Han, J. S. Martinez, and J. H. Werner, Nano Lett. **10**(8), 3106–3110 (2010).
[8]J. T. Petty, O. O. Sergev, D. A. Nicholson, P. M. Goodwin, B. Giri, and D. R. McMullan, Anal. Chem. **85**(20), 9868–9876 (2013).
[9]P. R. O'Neill, E. G. Gwinn, and D. K. Fygenson, J. Phys. Chem. C **115**(49), 24061–24066 (2011).
[10]M. Brust, M. Walker, D. Bethell, D. J. Schiffrin, and R. Whyman, J. Chem. Soc., Chem. Commun. **1994**(7), 801–802.
[11]S. Chen, R. S. Ingram, M. J. Hostetler, J. J. Pietron, R. W. Murray, T. G. Schaaff, J. T. Khoury, M. M. Alvarez, and R. L. Whetten, Science **280**(5372), 2098–2101 (1998).
[12]X. Kang and M. Zhu, Chem. Soc. Rev. **48**(8), 2422–2457 (2019).
[13]Y. Li and R. Jin, J. Am. Chem. Soc. **142**(32), 13627–13644 (2020).
[14]H. Häkkinen, Nat. Chem. **4**(6), 443–455 (2012).
[15]W. Hou, M. Dasog, and R. W. J. Scott, Langmuir **25**(22), 12954–12961 (2009).
[16]V. R. Jupally, R. Kota, E. V. Dornshuld, D. L. Mattern, G. S. Tschumper, D.-E. Jiang, and A. Dass, J. Am. Chem. Soc. **133**(50), 20258–20266 (2011).
[17]A. Henglein, P. Mulvaney, and T. Linnert, Faraday Discuss. **92**, 31–44 (1991).
[18]J. Zheng and R. M. Dickson, J. Am. Chem. Soc. **124**(47), 13982–13983 (2002).
[19]T. Yamane and N. Davidson, Biochim. Biophys. Acta **55**, 609–621 (1962).
[20]M. Daune, C. A. Dekker, and H. K. Schachman, Biopolymers **4**, 51–76 (1966).
[21]J. T. Petty, J. Zheng, N. V. Hud, and R. M. Dickson, J. Am. Chem. Soc. **126**(16), 5207–5212 (2004).
[22]C. M. Ritchie, K. R. Johnsen, J. R. Kiser, Y. Antoku, R. M. Dickson, and J. T. Petty, J. Phys. Chem. C **111**(1), 175–181 (2007).
[23]B. Sengupta, C. M. Ritchie, J. G. Buckman, K. R. Johnsen, P. M. Goodwin, and J. T. Petty, J. Phys. Chem. C **112**(48), 18776–18782 (2008).
[24]S. M. Copp, P. Bogdanov, M. Debord, A. Singh, and E. Gwinn, Adv. Mater. **26**(33), 5839–5845 (2014).
[25]D. Schultz and E. G. Gwinn, Chem. Commun. **48**(46), 5748–5750 (2012).
[26]J. T. Petty, B. Giri, I. C. Miller, D. A. Nicholson, O. O. Sergev, T. M. Banks, and S. P. Story, Anal. Chem. **85**(4), 2183–2190 (2013).
[27]J. T. Petty, M. Ganguly, A. I. Yunus, C. He, P. M. Goodwin, Y.-H. Lu, and R. M. Dickson, J. Phys. Chem. C **122**(49), 28382–28392 (2018).
[28]J. T. Petty, O. O. Sergev, M. Ganguly, I. J. Rankine, D. M. Chevrier, and P. Zhang, J. Am. Chem. Soc. **138**(10), 3469–3477 (2016).
[29]D. Schultz, K. Gardner, S. S. R. Oemrawsingh, N. Markešević, K. Olsson, M. Debord, D. Bouwmeester, and E. Gwinn, Adv. Mater. **25**, 2797–2803 (2013).
[30]M. S. Blevins, D. Kim, C. M. Crittenden, S. Hong, H.-C. Yeh, J. T. Petty, and J. S. Brodbelt, ACS Nano **13**(12), 14070–14079 (2019).
[31]D. J. E. Huard, A. Demissie, D. Kim, D. Lewis, R. M. Dickson, J. T. Petty, and R. L. Lieberman, J. Am. Chem. Soc. **141**(29), 11465–11470 (2019).
[32]C. Cerretani, H. Kanazawa, T. Vosch, and J. Kondo, Angew. Chem., Int. Ed. **58**, 17153 (2019).
[33]R. R. Ramazanov, T. S. Sych, Z. V. Reveguk, D. A. Maksimov, A. A. Vdovichev, and A. I. Kononov, J. Phys. Chem. Lett. **7**(18), 3560–3566 (2016).
[34]D. Schultz, R. G. Brinson, N. Sari, J. A. Fagan, C. Bergonzo, N. J. Lin, and J. P. Dunkers, Soft Matter **15**(21), 4284–4293 (2019).
[35]A. Gonzàlez-Rosell, C. Cerretani, P. Mastracco, T. Vosch, and S. M. Copp, Nanoscale Adv. **3**(5), 1230–1260 (2021).
[36]Y. Zhang, C. He, J. T. Petty, and B. Kohler, J. Phys. Chem. Lett. **11**(21), 8958–8963 (2020).
[37]S. A. Patel, M. Cozzuol, J. M. Hales, C. I. Richards, M. Sartin, J.-C. Hsiang, T. Vosch, J. W. Perry, and R. M. Dickson, J. Phys. Chem. C **113**(47), 20264–20270 (2009).
[38]C. Cerretani, M. R. Carro-Temboury, S. Krause, S. A. Bogh, and T. Vosch, Chem. Commun. **53**(93), 12556–12559 (2017).
[39]C. He, P. M. Goodwin, A. I. Yunus, R. M. Dickson, and J. T. Petty, J. Phys. Chem. C **123**(28), 17588–17597 (2019).
[40]J. T. Petty, C. Fan, S. P. Story, B. Sengupta, M. Sartin, J.-C. Hsiang, J. W. Perry, and R. M. Dickson, J. Phys. Chem. B **115**(24), 7996–8003 (2011).
[41]E. Thyrhaug, S. A. Bogh, M. R. Carro-Temboury, C. S. Madsen, T. Vosch, and D. Zigmantas, Nat. Commun. **8**, 15577 (2017).
[42]Z. Reveguk, R. Lysenko, R. Ramazanov, and A. Kononov, Phys. Chem. Chem. Phys. **20**(44), 28205–28210 (2018).
[43]S. A. Bogh, M. R. Carro-Temboury, C. Cerretani, S. M. Swasey, S. M. Copp, E. G. Gwinn, and T. Vosch, Methods Appl. Fluoresc. **6**(2), 024004 (2018).
[44]D. Andreatta, J. L. Pérez Lustres, S. A. Kovalenko, N. P. Ernsting, C. J. Murphy, R. S. Coleman, and M. A. Berg, J. Am. Chem. Soc. **127**(20), 7270–7271 (2005).
[45]R. Jimenez, G. R. Fleming, P. V. Kumar, and M. Maroncelli, Nature **369**(6480), 471–473 (1994).
[46]I. H. M. van Stokkum, D. S. Larsen, and R. van Grondelle, Biochim. Biophys. Acta, Bioenerg. **1657**(2-3), 82–104 (2004).
[47]T. Vosch, Y. Antoku, J.-C. Hsiang, C. I. Richards, J. I. Gonzalez, and R. M. Dickson, Proc. Natl. Acad. Sci. U. S. A. **104**(31), 12616–12621 (2007).
[48]J. T. Petty, C. Fan, S. P. Story, B. Sengupta, A. St. John Iyer, Z. Prudowsky, and R. M. Dickson, J. Phys. Chem. Lett. **1**(17), 2524–2529 (2010).
[49]I. L. Volkov, P. Y. Serdobintsev, and A. I. Kononov, J. Phys. Chem. C **117**(45), 24079–24083 (2013).
[50]N. J. Turro, V. Ramamurthy, and J. C. Scaiano, *Modern Molecular Photochemistry of Organic Molecules* (Science Books, 2010).
[51]Z. K. Wu and R. C. Jin, Nano Lett. **10**(7), 2568–2573 (2010).
[52]M. Walter, J. Akola, O. Lopez-Acevedo, P. D. Jadzinsky, G. Calero, C. J. Ackerson, R. L. Whetten, H. Gronbeck, and H. Häkkinen, Proc. Natl. Acad. Sci. U. S. A. **105**(27), 9157–9162 (2008).
[53]M. Pelton, Y. Tang, O. M. Bakr, and F. Stellacci, J. Am. Chem. Soc. **134**(29), 11856–11859 (2012).
[54]S. H. Yau, B. A. Ashenfelter, A. Desireddy, A. P. Ashwell, O. Varnavski, G. C. Schatz, T. P. Bigioni, and T. Goodson, J. Phys. Chem. C **121**(2), 1349–1361 (2017).
[55]V. Soto-Verdugo, H. Metiu, and E. Gwinn, J. Chem. Phys. **132**(19), 195102 (2010).
[56]R. Longuinhos, A. D. Lúcio, H. Chacham, and S. S. Alexandre, Phys. Rev. E **93**(5), 052413 (2016).
[57]M. A. Filatov, S. Baluschev, and K. Landfester, Chem. Soc. Rev. **45**(17), 4668–4689 (2016).